Properties of SiO_2–M_xO_y Composites Doped with the Europium(III) Di(1,10-phenanthroline) Complex

Huihui Li, Daisuke Ueda, Satoshi Inoue, Ken-ichi Machida,*,† and Gin-ya Adachi*

Department of Applied Chemistry, Graduate school of Engineering, Osaka University,
2-1 Yamadaoka, Suita, Osaka 565-0871

†Collaborative Research Center for Advanced Science and Technology, Osaka University,
2-1 Yamadaoka, Suita, Osaka 565-0871

(Received February 8, 2001)

The europium(III) 1,10-phenanthroline complex ([Eu(phen)$_2$]Cl$_3$) was doped into the SiO_2–M_xO_y xerogel matrices derived from tetraethyl orthosilicate (TEOS) and metal alkoxides (M(OR)$_n$, M = Zr, Ta) by the sol-gel method. The resultant composites were characterized by X-ray diffraction, luminescence, UV-visible, and FT-IR spectroscopic measurements. In addition, phonon sideband (PSB) and luminescence quantum efficiency measurements have been conducted on some of the (SiO_2–ZrO_2):Eu(phen)$_2{}^{3+}$ composites. The luminescence emission intensity of the (SiO_2–M_xO_y):Eu(phen)$_2{}^{3+}$ composites was found to be dependent on the matrix composition, i.e. the emission intensity maximized at the matrix composition of Si:M = 9:1. This observation was interpreted from various factors, such as the –OH groups in the matrices, the UV-absorbance and coupling with the lattice-vibration of the host matrices, and the non-radiative energy transfer between the neighboring Eu^{3+} ions, that affect the luminescence intensities of the resultant composites.

The sol-gel method has been established as a handy approach for the preparation of various glass and ceramic composite materials doped with organic or organometallic compounds, which are susceptible to high temperatures. To date, this method has found extensive applications in various fields, such as solid tunable lasers,[1–5] non-linear optical materials,[6,7] luminescent solar concentrators,[8,9] and other materials.[10–13]

In our previous work, the lanthanide complexes, e.g. [Eu(phen)$_2$]Cl$_3$ and [Tb(bpy)$_2$]Cl$_3$, have been doped into the silica matrices as derived from tetraethyl orthosilicate (TEOS) by the sol-gel process.[14,15] The thermal stability of the complexes was improved by the incorporation into the solid matrices and the mechanical properties of the resultant composite materials were also strengthened. However, the emission intensities of the resultant composite materials were low, because only small amounts of the complexes could be doped into the silica matrices to result in composite products with good transparent appearances. In order to obtain inorganically based composites with high emission intensities, it is necessary to develop matrices which are capable of incorporating large amounts of the complex dopants.

On the other hand, as suggested by Avnir,[16] metal oxides derived from metal alkoxides as starting materials, e.g. TiO_2, ZrO_2, Ta_2O_5, and Al_2O_3, may be also employed as the hosts for such composites materials. As a matter of fact, some of the metal oxide materials prepared by the sol-gel method have been reported to possess good optical properties.[17,18] Since the reactivities of metal alkoxides in hydrolysis and polycondensation are known to be much higher than TEOS,[19] the high gelation rate of the sols containing metal alkoxides may promote the trapping of the dopant in solid matrices. Moreover, the partial substitution of SiO_2 units by metal oxide ones is expected to result in the downshift of lattice vibration and thus, depression of the multiphonon relaxation for the complex dopant through the coupling with the lattice vibration which is anticipated. It is of interest to investigate the potential of using these oxides or their composites with SiO_2 as hosts to dope lanthanide complexes into inorganic matrices.

The present paper reports the preparation and properties of the [Eu(phen)$_2$]Cl$_3$ complex-dispersed SiO_2–M_xO_2 (M = Zr, Ta) composites. The resultant composites were characterized by a series of spectroscopic measurements and the variation in their luminescence intensities was discussed.

Experimental

The [Eu(phen)$_2$]Cl$_3$ complex was synthesized according to the procedures described previously.[15] Mixtures consisted of TEOS (99.9%, Wako Pure Chemical Industries, Ltd.), C_2H_5OH, and H_2O (deionized one) in a molar ratio of 1:10:1 were refluxed for 1 h, using a few drops of diluted HCl solution as the catalyst. Then, appropriate amounts of Zr(O-n-C_4H_9)$_4$ (85.0–90.0%, Kanto Chemical Co., Inc.) or Ta(OC_2H_5)$_5$ (99.9%, Wako Pure Chemical Industries, Ltd.) were added to the resultant solutions, these mixtures were refluxed together for another 1 h to give clear sol precursor solutions. Subsequently, appropriate amounts of [Eu(phen)$_2$]Cl$_3$, H_2O, and dimethylformamide (DMF, 99.9%) were mixed and added to the precursor solutions obtained as above. The resultant mixtures with molar ratios of (Si+M):[Eu(phen)$_2$]Cl$_3$:H_2O:DMF = 1:y:4:1 (y = 0.01–0.2) were magnetically stirred together for a few minutes until they became homogeneous. Finally, the complex-dispersed solutions were cast into polystyrene cuvettes (33 mmϕ×55 mm) and cured at 50 °C in air for about 10–14 days to give [Eu(phen)$_2$]Cl$_3$-doped composite xerogels. The xerogel samples were further heated at 200 °C for 5 h in air before measurements.

The (SiO$_2$–M$_x$O$_y$):Eu(phen)$_2^{3+}$ composites have been characterized by luminescence, XRD, UV-visible, and FT-IR spectroscopy. Moreover, phonon sideband (PSB) spectra and luminescence quantum efficiency values of some of the (SiO$_2$–ZrO$_2$):Eu(phen)$_2^{3+}$ composites were also measured. The luminescence spectra were recorded on a Hitachi fluorescence spectrophotometer Model F-4500 equipped with xenon lamp as the light resource, using the "front face" orientation. All the spectra have been corrected. The relative emission intensities were calculated by comparing the integrated area of the emission bands of the composite samples to that of a commercially available red lamp phosphor Y(P, V)O$_4$:Eu, as has been described previously.[20] The UV-visible spectra were recorded on a Shimadzu double beam spectrophotometer Model UV 2200. FT-IR spectra were measured on a JAS FT/IR-430 spectrophotometer by the KBr method. The phonon sideband spectra have been obtained as associated with the $^7F_0 \rightarrow {}^5D_2$ transition of Eu^{3+} in the excitation spectrum. Using a method developed by Okubo et al.,[21] the absolute fluorescent quantum efficiencies of the composites were determined by a polychromator, which were calibrated by a conical cavity thermal radiation detector. The effective spectral absorptance of the detector was constant with 0.3% over a wavelength of 200–600 nm. Reproducibility of the absolute fluorescent quantum efficiency was within ± 0.5%.

Results and discussion

The [Eu(phen)$_2$]Cl$_3$ complex was doped into the M$_x$O$_y$ (M = Zr and Ta) composite xerogels with various compositions by the sol-gel technique, using TEOS and zirconium tetrabutoxide (Zr(O-n-C$_4$H$_9$)$_4$) or tantalum pentaethoxide (Ta(OC$_2$H$_5$)$_5$) as the starting materials. The obtained composites were amorphous, as evidenced by XRD measurements. In addition, it was found that the gelation of the sol solutions containing metal alkoxides was greatly facilitated in comparison with that of the sols containing TEOS only, as indicated in Fig. 1. This is well in accordance with our expectation of the rapid evolution of the sols derived from the alkoxide mixtures containing highly active metal alkoxides.

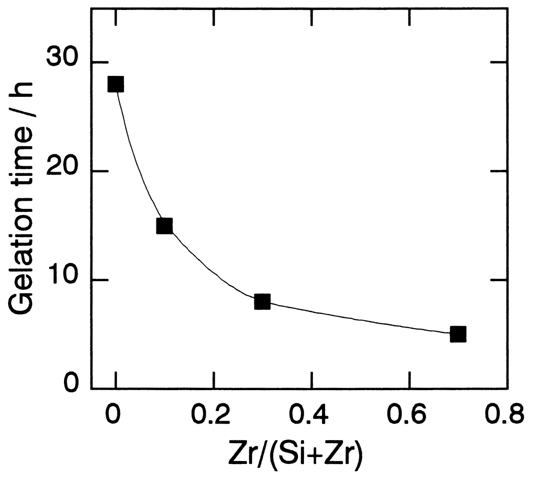

Fig. 1. Gelation times for the sols containing alkoxide mixtures with various compositions.

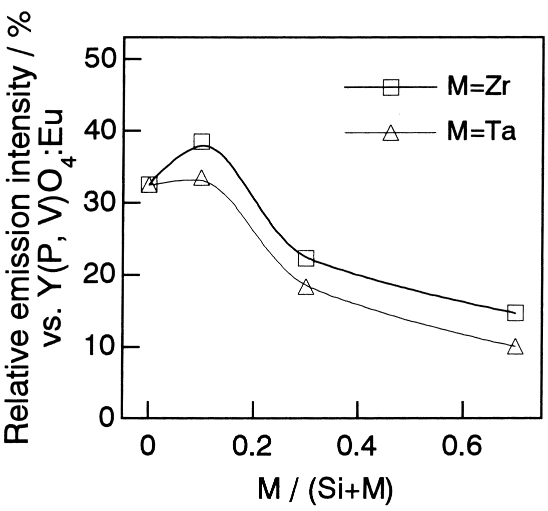

Fig. 2. Compositional dependencies of the emission intensity for the (SiO$_2$–M$_x$O$_y$):Eu(phen)$_2^{3+}$ composites (M = Zr, Ta) doped with 3 mol% of the complex.

All of the (SiO$_2$–M$_x$O$_y$):Eu(phen)$_2^{3+}$ composites provided intense red emission lines of Eu^{3+} ions under UV light irradiation. The luminescence intensities of the composites doped with 3 mol% of the [Eu(phen)$_2$]Cl$_3$ complex are presented in Fig. 2 as a function of the matrix composition. Obviously, the emission intensity maximizes at the matrix composition of Si:M = 9:1 for both the (SiO$_2$–ZrO$_2$):Eu(phen)$_2^{3+}$ and the (SiO$_2$–Ta$_2$O$_5$):Eu(phen)$_2^{3+}$ composites, in spite of the variation of the metal oxide component in the matrices. This behavior is similar to the result that has been observed on the (SiO$_2$–M$_x$O$_y$):Tb(bpy)$_2^{3+}$ composites.[22] We at first assumed that the main reason for this observation might be ascribed to the variation of the local chemical environment surrounding the Eu^{3+} ions as the host matrix composition was changed, because the ratio of the peak intensity of the $^5D_0 \rightarrow {}^7F_2$ transition (615 nm) to that of $^5D_0 \rightarrow {}^7F_1$ (595 nm), here denoted as I_{615}/I_{595}, can be considered as an indication of the local asymmetry of the Eu^{3+} ions.[23] The I_{615}/I_{595} values for the present (SiO$_2$–M$_x$O$_y$):Eu(phen)$_2^{3+}$ composites have been calculated and the results are shown in Fig. 3 as a function of the matrix composition. However, unlike the previous ORMOSIL:Eu(phen)$_2^{3+}$ composites,[24] there seems to be no close correlation between the I_{615}/I_{595} ratios and the luminescence emission intensities with the matrix composition. This behavior implies that other factors in addition to the asymmetry of the Eu^{3+} ions have influential impacts on the emission intensities of the (SiO$_2$–M$_x$O$_y$):Eu(phen)$_2^{3+}$ composites.

Luminescence lifetimes and the quantum efficiencies of the (SiO$_2$–ZrO$_2$):Eu(phen)$_2^{3+}$ (3 mol%) composites have been measured and the values are summarized in Table 1, together with the radiative decay rate constant and non-radiative decay rate constant calculated according to equations 1 and 2:[25]

$$\phi = A_{\mathrm{rad}}\tau \qquad (1)$$

$$1/\tau = A_{\mathrm{rad}} + W_{\mathrm{nr}} \qquad (2)$$

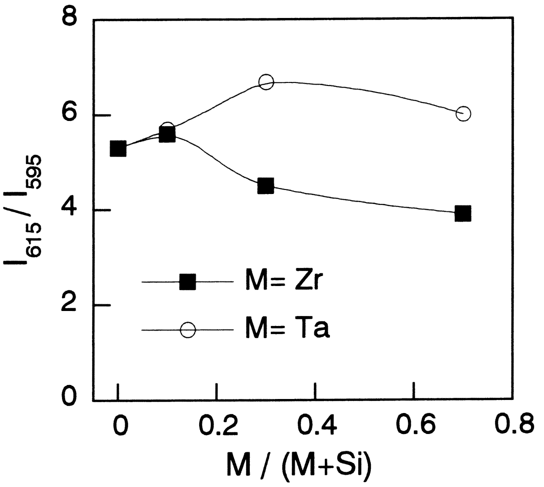

Fig. 3. Peak intensity ratios (I_{615}/I_{595}) as a function of the matrix composition for the $(SiO_2–M_xO_y)$: $Eu(phen)_2^{3+}$ (3 mol%) composites (M = Zr, Ta).

Table 1. Luminescence Properties of $(SiO_2–ZrO_2)$: $Eu(phen)_2^{3+}$ (3 mol%) Composites Based on Various Matrix Compositions

Si : Zr	ϕ*(%)	τ (μs)	A_{rad} ($\times 10^2$ s^{-1})	W_{nr} ($\times 10^2$ s^{-1})
10 : 0	23	674.1	3.4	1.1
9 : 1	24	683.6	3.5	1.1
7 : 3	13	470.4	3.2	1.8
3 : 7	10	438.8	2.3	2.0

* Measured at the excitation wavelength of 335 nm.

In the above equations, ϕ is the quantum efficiency; τ stands for the luminescence lifetime, while A_{rad} and W_{nr} denote the radiative and non-radiative decay rate constants, respectively. Apparently, the non-radiative decay rate constant is several times larger than the radiative one for all of the samples and thus has great influence on the quantum efficiencies of the composites. The W_{nr} value is the smallest for the composites with Si : Zr $\geq$ 9 : 1, and hence these composites have the lowest non-radiative decay probabilities through multi-phonon relaxation processes. As a result, the quantum efficiencies are comparable for the composites with 0 and 0.1 molar fractions of ZrO_2. On the other hand, the non-radiative multiphonon decay probabilities for the composites with the higher fractions of ZrO_2 are remarkably increased in comparison with those of the lower ZrO_2 contents, contributing to the prominent decrease of the quantum efficiencies for the corresponding composites.

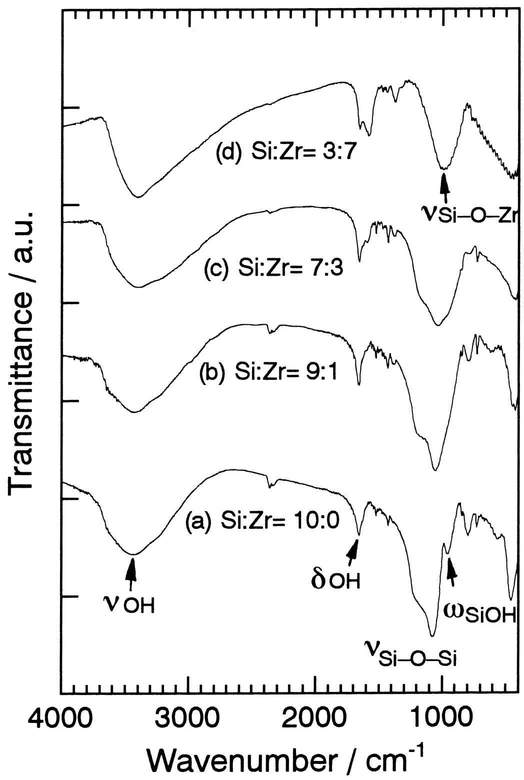

Fig. 4. FT-IR spectra of the $(SiO_2–ZrO_2)$: $Eu(phen)_2^{3+}$ (3 mol%) composites based on matrices with various Si : Zr ratios: (a) 10 : 0, (b) 9 : 1, (c) 7 : 3, and (d) 3 : 7.

FT-IR spectra of the $(SiO_2–M_xO_y)$: $Eu(phen)_2^{3+}$ composites have been also recorded. The spectrum patterns recorded on the $(SiO_2–ZrO_2)$: $Eu(phen)_2^{3+}$ (3 mol%) ones are shown in Fig. 4. The absorption assigned to –OH stretching (νOH: ~3400 cm^{-1}) and flexion (δOH: ~1650 cm^{-1}) modes are of comparable intensities for the composites with the ZrO_2 fractions of 0.1 or below it, while they have drastically strengthened for the composites with the higher ZrO_2 fractions. It is believed that many more –OH groups are remaining in the composites with higher ZrO_2 contents. Consequently, the non-radiative multiphonon relaxation due to such –OH stretching must be prominent for the composites with ZrO_2 fractions of 0.3 or higher, in accordance with the results listed in Table 1. On the other hand, the lattice vibration mode shifts to the lower wavenumber side as the ZrO_2 content is raised in the matrices. The lattice vibrations are dominated by symmetric and anti-symmetric Si–O–Si stretching modes (ν_sSi–O–Si and ν_{as}Si–O–Si) when the ZrO_2 molar fraction is 0.1 or below it. However, when the ZrO_2 content is increased to 0.3 or above it, the lattice vibrations apparently becomes characteristic of those of νSi–O–Zr (~950–970 cm^{-1}). This indicates the successful formation of the $SiO_2–ZrO_2$ composite matrices. Similar experimental results were obtained on the $(SiO_2–Ta_2O_5)$: $Eu(phen)_2^{3+}$ composites.

The coupling with the lattice vibration is one of the factors that lead to the non-radiative decay for the Eu^{3+} ions. The coupling strength of the phonons with the electrons of Eu^{3+} ions can be evaluated by measuring the phonon sideband spectra.[25,26] The pure electronic transition of a Eu^{3+} ion can be accompanied by the cooperative vibrational transitions of some lattice units in the surroundings of the ion. As a result, if we monitor the emission of the Eu^{3+} ion, such phonon sidebands can be observed in the high energy region to the pure electronic transition of the Eu^{3+} ion.[26] The PSB spectra of the present $(SiO_2–ZrO_2)$: $Eu(phen)_2^{3+}$ composites have been obtained in their excitation spectra by association with the $^7F_0 – {}^5D_2$ transition of Eu^{3+} ions, as shown in Fig. 5. Practically, the electron-phonon coupling strength (g) can be evaluated by comparing the integrated area of the PSB peak to that assigned to the pure electronic the $^7F_0 – {}^5D_2$ transition of the Eu^{3+} ion itself. The

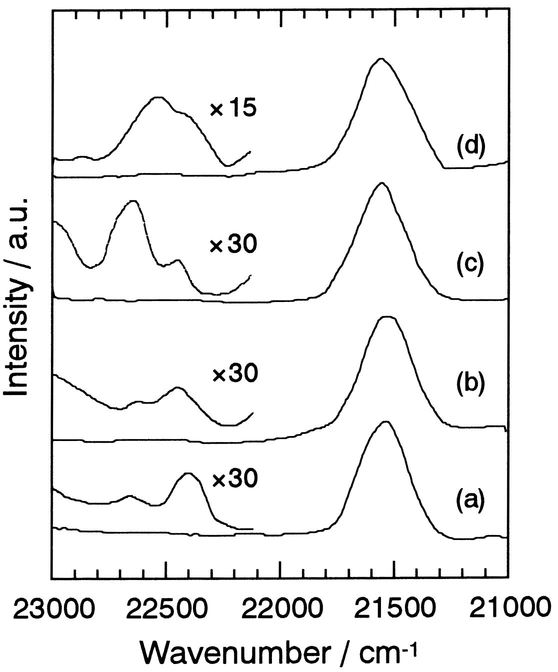

Fig. 5. Phonon sideband spectra of the (SiO_2–ZrO):Eu(phen)$_2^{3+}$ (3 mol%) composites based on matrices with various Si:Zr ratios: (a) 10:0, (b) 9:1, (c) 7:3, and (d) 3:7. The PSB spectra have been obtained as associated with the $^7F_0$ – $^5D_2$ transition of Eu^{3+} ion.

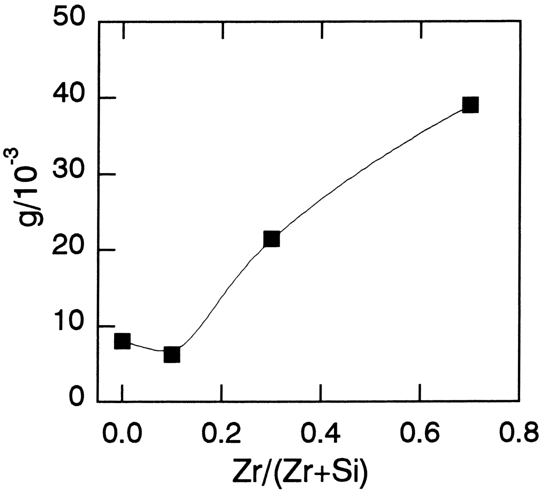

Fig. 6. The electron-phonon coupling strength for the (SiO_2–ZrO_2):Eu(phen)$_2^{3+}$ composites (3 mol%) with various matrix compositions.

calculated electron-phonon coupling strength values have been plotted as a function of the matrix composition as shown in Fig. 6. Once again, the coupling strength is comparable for the composites with 0.1 molar fraction of ZrO_2 or below it, while it is greatly increased as the ZrO_2 content is increased to be above 0.3. The non-radiative decay probability caused by the lattice vibration then is greatly enhanced for the composites based on the matrices of 0.3 molar fraction of ZrO_2 or above it, in spite of the downshift of the lattice vibration energy as the ZrO_2 content in the matrix is increased.

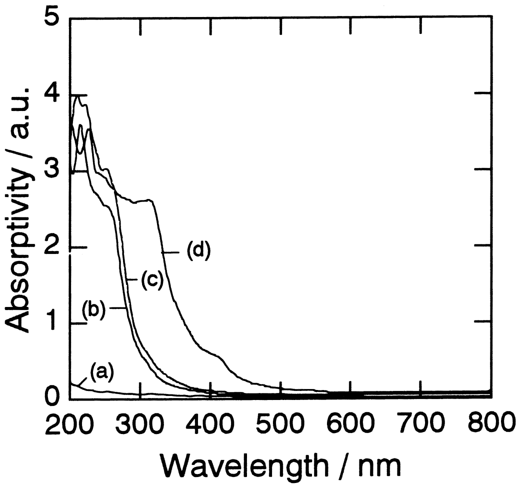

Fig. 7. The UV-visible absorption spectra of the sol-gel-derived SiO_2–ZrO_2 composite matrices (ca. 2 mm in thickness) with various Si:Zr ratios: (a) 10:0, (b) 9:1, (c) 7:3, and (d) 3:7.

In addition, we have measured the UV-visible absorption spectra of the SiO_2–M_xO_y matrices based on various compositions. Typical spectrum patterns of the SiO_2–ZrO_2 ones are shown in Fig. 7 for instance. Apparently, the absorbance below 400 nm increases drastically with increasing the metal oxide content in the matrices. As a result, the UV light intensities for exciting the complex molecules are supposed to be decreased, leading to the decrease in the emission intensity for the (SiO_2–M_xO_y):Eu(phen)$_2^{3+}$ composites as the M_xO_y component in the matrices is increased.

Various amounts of the [Eu(phen)$_2$]Cl_3 complex were doped into matrices with the matrix composition of Si:Zr = 9:1. In comparison with the sol-gel derived silica matrix which could incorporate at most 3–5% of the complex to give out transparent composites,[14,15] as high as ~20 mol% of the complex was doped into the SiO_2–ZrO_2 composite matrices and the process still resulted in composite phosphors with good transparency. This must be ascribed to the faster gelation of the precursor sol solutions containing highly reactive metal alkoxides, as indicated in Fig. 1. Consequently, the complex molecules are efficiently trapped more homogeneously in the SiO_2–ZrO_2 (Si:Zr = 9:1) composite matrix than in the single-component SiO_2 matrix only. The phase separation and/or precipitation of the complex, which are closely related to the increased viscosity of the sol solutions and the inhibition on the diffusion of the complex due to the vaporization of the solvents, can thus be effectively prevented.

The dependence of the emission intensities for the (SiO_2–ZrO_2):Eu(phen)$_2^{3+}$ (Si:Zr = 9:1) composites on the dopant concentration is shown in Fig. 8. The emission intensity of the composites gradually increases with an elevation of the complex concentration and maximizes at ~78% vs Y(P, V)O_4:Eu with the concentration of 15–20 mol%. No apparent luminescence concentration quenching effect was observed, confirming the good dispersion of the complex dopant in the composite matrix.

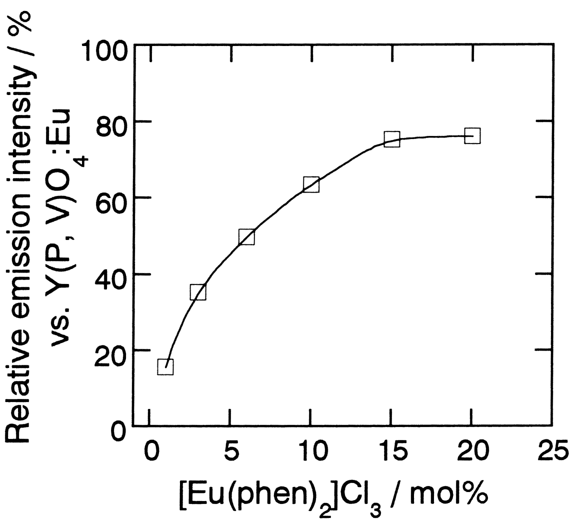

Fig. 8. Emission intensities of the (SiO_2–ZrO_2):Eu(phen)$_2^{3+}$ (Si:Zr = 9:1) composites as a function of the [Eu(phen)$_2$]-Cl_3 concentration.

The observation that the emission intensity of the (SiO_2–M_xO_y):Eu(phen)$_2^{3+}$ composites maximizes at the matrix composition of Si:M = 9:1 (see Fig. 2) was discussed based on the various factors that affect the emission intensities of the composites. As indicated in Figs. 4 and 6, both the –OH vibrational intensity and the electron–phonon coupling strength of the composites increase with elevating the metal oxide content. Therefore, the emission intensity of the composites tends to decrease as the probabilities of the non-radiative decay through –OH vibrations and coupling with the lattice vibration are increased. In addition, the UV-absorbance of the composite matrices increases with the metal oxide content, leading to the reduction of the excitation energy for the complex dopant and consequentially the tendency of a decrease in the emission intensity. On the other hand, if we take the rapid gelation and the comparatively more homogeneous dispersion of the complex in the composite matrix into consideration, this will result in the depression of the non-radiative relaxation through energy transfer between neighboring lanthanide complexes. Consequently, the emission intensity tends to increase with the metal oxide content. Therefore, the observation that the emission intensity maximizes at the matrix composition of Si:M = 9:1 for the (SiO_2–M_xO_y):Eu(phen)$_2^{3+}$ composites should be ascribed to the comprehensive influences from the above factors which affect the emission intensity of the composites.

Conclusions

Luminescent composite materials showing intense red emission lines under UV light irradiation have been obtained by doping the [Eu(phen)$_2$]Cl_3 complex into the SiO_2–M_xO_y (M = Zr, Ta) composite matrices through the sol-gel method. The emission intensity of the resultant (SiO_2–M_xO_y):Eu(phen)$_2^{3+}$ composite phosphors is strongly dependent on the matrix composition, maximizing at Si:M = 9:1. This observation is ascribed to the comprehensive influences from the remaining –OH groups in the matrices, the UV-absorbance and coupling with the lattice-vibration of the host matrices, and the depressed non-radiative energy transfer between the neighboring Eu^{3+} ions with an elevation of the M_xO_y content.

Owing to the rapid gelation of the sol precursor solutions containing reactive metal alkoxide, the (SiO_2–ZrO_2):Eu(phen)$_2^{3+}$ (Si:Zr = 9:1) composites with good transparency have been obtained in spite of the high complex doping concentrations of up to ~20 mol%. As a result, the emission intensity of the (SiO_2–ZrO_2):Eu(phen)$_2^{3+}$ composite phosphors obtained under the optimized preparation conditions maximizes at ~78% vs Y(P, V)O_4:Eu.

The authors of this work would like to acknowledge the Japan Society for the Promotion of Science and the Ministry of Education, Science, Sports and Culture for their financial support. In addition, the authors are grateful to Dr. Kazuaki Okubo and Dr. Tomizo Matsuoka of Matsushita Electric Industrial Co., Ltd. for their support in measuring the quantum efficiencies of the (SiO_2–ZrO_2):Eu(phen)$_2^{3+}$ composites.

References

1 F. Salin, G. Le Saux, P. Georges, A. Brun, C. Bagnall, and J. Zarzycki, *Opt. Lett.*, **14**, 785 (1989).

2 J. C. Altman, R. E. Stone, F. Nishida, and B. Dunn, *Sol-Gel Optics II. SPIE,* **507**, 1758 (1992).

3 R. Reisfeld, R. Gvishi, and Z. Burshtein, *J. Sol.-Gel Sci. Technol.*, **4**, 49 (1995).

4 H. Law, T. Tou, and S. Ng, *Appl. Opt.*, **37**, 5694 (1998).

5 L. Hu and Z. Jiang, *Opt. Commun.*, **148**, 275 (1998).

6 H. Kim, J. L. Plawsky, R. Lapuerta, and G. M. Korenowski, *Chem. Mater.*, **4**, 249 (1992).

7 D. H. Choi, J. H. Park, T. H. Rhee, N. Kim, and S. Lee, *Chem. Mater.*, **10**, 705 (1998).

8 R. Reisfeld, D. Shamrakov, and C. Jorgensen, *Solar Energy Mater. Solar Cells*, **33**, 417 (1994).

9 K. Machida, H. Li, D. Ueda, S. Inoue, and G. Adachi, *J. Lumin.*, **87-89**, 1257 (2000).

10 R. Reisfeld, *J. Non-Cryst. Solids*, **121**, 254 (1990).

11 P. Tien and L. Chau, *Chem. Mater.*, **11**, 2141 (1999).

12 M. Nogami, T. Nagakura, and T. Hayakawa, *J. Phys.: Condens. Matter*, **10**, 1 (1998).

13 S. G. Kulikov, A. V. Veret-Lemarinier, J. P. Galaup, F. Chaput, and J. P. Boilot, *Chem. Phys.*, **216**, 147 (1997).

14 T. Jin, S. Tsutsumi, Y. Deguchi, K. Machida, and G. Adachi, *J. Electrochem. Soc.*, **142**, 195 (1995).

15 T. Jin, S. Tsutsumi, Y. Deguchi, K. Machida, and G. Adachi, *J. Alloys Compds.*, **252**, 59 (1997).

16 D. Avnir, *Acc. Chem. Res.*, **28**, 328 (1995).

17 D. R. Uhlmann, J. M. Boulton, G. Teowee, L. Wesenbach, and B. J. Zelinski, *J. Sol-Gel Opt., SPIE*, **1328**, 270 (1990).

18 H. Krug, F. Tiefensee, P. W. Oliveira, and H. Schmidt, *Sol-Gel Opt., SPIE*, **1758**, 448 (1992).

19 N. Yamada, I. Yoshinaga, and S. Katayama, *J. Mater. Chem.*, **7**, 1491 (1997).

20 H. Li, S. Inoue, K. Machida, and G. Adachi, *Chem. Mater.*, **11**, 3171 (1999).

21 K. Okubo and T. Shigeta, *J. Illum. Engng. Inst. Jpn.*, **83**, 87 (1999).

22 H. Li, S. Inoue, D. Ueda, K. Machida, and G. Adachi, *J. Ceram. Soc. Jpn.*, **108**, 325 (2000).

23 X. Fan, M. Wang, and G. Xiong, *Mater. Sci. Eng.*, **B21**, 55

(1993).
24 H. Li, S. Inoue, D. Ueda, K. Machida, and G. Adachi, *Bull. Chem. Soc. Jpn.*, **73**, 258 (2000).
25 H. Toratani, T. Izumitani, and H. Kuroda, *J. Non-Cryst. Solids*, **52**, 303 (1982).
26 S. Tanabe, S. Todoroki, K. Hirao, and N. Soga, *J. Non-Cryst. Solids*, **122**, 59 (1990).